JCB
J Circ Biomark 2026; 15: 47-57
ISSN 1849-4544 | DOI: 10.33393/jcb.2026.3840
ORIGINAL RESEARCH ARTICLE

Circulating miRNAs (135a-5p, 646 AND 1271-5P) in Breast Cancer Diagnosis and Staging: Integrative Network and Functional Analysis

Asmaa R Abdel-Hamed[1], Marina Barsom[2], Mahmoud M Kamel[3], Dina M Abo-Elmatty[1], Abdullah AY Gibriel[2]

[1]Department of Biochemistry, Faculty of Pharmacy, Suez Canal University, Ismailia - Egypt
[2]Pharmacology & Biochemistry Department, Biochemistry & Molecular Biology Division, Faculty of Pharmacy, The British University in Egypt (BUE), El Sherouk City, Cairo Governorate - Egypt
[3]Clinical Pathology Department, National Cancer Institute, Cairo University, Cairo - Egypt

ABSTRACT

Introduction: Breast cancer (BC) remains a leading cause of cancer-related mortality among women worldwide. Despite advances in molecular diagnostics, reliable non-invasive biomarkers for early detection and disease staging remain limited. Circulating microRNAs (miRNAs) are promising epigenetic regulators involved in tumor development and progression.

Methods: Determination of plasma miRNA (1271-5p, miR-646, and miR-135a-5p) differential expression profiles in an Egyptian cohort comprising 111 BC patients (stages 0–IV), 25 benign breast disease cases, and 24 healthy controls. Their diagnostic and stage-specific performance was assessed alongside integrative analyses of predicted and validated biological targets with network construction.

Results: miR-1271-5p was downregulated in benign tumors but overexpressed across all BC stages. miR-646 was generally downregulated, with a notable increase in stage III, whereas miR-135a-5p was elevated in benign and early-stage disease before declining in metastatic stage IV. ROC analyses demonstrated strong discriminatory performance, with miR-1271-5p distinguishing early-stage BC from controls and benign lesions, miR-646 separating benign/early malignant cases from controls, and miR-135a-5p identifying metastatic disease. Combined miRNA panels improved discrimination between malignant and non-malignant samples and between early and advanced stages. Integrative analyses identified putative regulation of ZEB1, CCND2, FOXN3, and RUNX2, while TP53TG1, ZFAS1, XIST, and MALAT1 emerged as potential interaction hubs. Functional enrichment suggested involvement in AMPK, FOXO, SUMOylation, TP53-mediated, and immune-related pathways.

Conclusions: Circulating miR-1271-5p, miR-646, and miR-135a-5p, individually and in combination, show promise as non-invasive diagnostic and stage-specific biomarkers for BC. Integrative network analyses provide insight into their putative roles in BC progression.

Keywords: Breast cancer, Non-invasive Biomarkers, staging, miR-1271-5p, miR-646, miR-135a-5p, MALAT1, FOXO

Introduction

Breast cancer (BC) is the second most prevalent cancer globally, and the fourth highest cause of cancer death in the world. It accounts for approximately 25% of all female cancer diagnoses and remains a major public health challenge due to its increasing incidence and mortality rates (1). In Egypt, BC is the most prevalent cancer among women, with over 22,000 new cases and more than 9,000 related deaths reported annually, and incidence rates are expected to rise substantially in the coming decades (2).

Breast cancer (BC) is a heterogeneous disease that progresses through stages 0–IV, ranging from localized lesions to metastatic disease. Early diagnosis remains essential for improving therapeutic outcomes and survival. Current diagnostic approaches, including mammography, ultrasound, magnetic resonance imaging, and tissue biopsy, have important limitations such as reduced sensitivity in dense breast tissue, operator dependency, high cost, invasiveness, and potential diagnostic inaccuracies (3). Furthermore, conventional serum biomarkers, including carcinoembryonic antigen (CEA) and cancer antigen 15-3 (CA15-3), demonstrate limited sensitivity and inconsistent clinical utility (4). These limitations highlight the need for accurate, minimally invasive biomarkers capable of supporting early detection and disease staging.

Received: June 7, 2026
Accepted: August 16, 2026
Published online: September 15, 2026

This article includes supplementary material

Corresponding author:
Abdullah AY Gibriel
email: abdullah.gibriel@bue.edu.eg

Liquid biopsy has emerged as a promising diagnostic approach through the detection of circulating biomarkers in body fluids. Among these biomarkers, microRNAs (miRNAs) are small non-coding RNAs (18-25 nucleotides) that regulate gene expression by targeting messenger RNAs and modulating diverse cellular processes, including proliferation, differentiation, apoptosis, invasion, and metastasis. Their remarkable stability in circulation and cancer-specific expression patterns make them attractive candidates for non-invasive cancer diagnosis and prognosis (5-8).

MicroRNAs (miRNA) (miR-1271-5p, miR-646, and miR-135a-5p) were selected based on accumulating evidence implicating them in cancer development and progression through regulation of key hallmarks of cancer. For instance, miR-1271-5p functions predominantly as a tumor suppressor in lung adenocarcinoma, glioma, cervical cancer, and multiple myeloma by targeting FRS2, HK2, FLOT1, and SOX13, thereby regulating glycolysis, epithelial–mesenchymal transition (EMT), and the Wnt/β-catenin signaling pathway (9-12). Similarly, miR-135a-5p suppresses tumor progression in BC, glioma, gallbladder cancer, and head and neck squamous cell carcinoma through regulation of BAG3, ANGPT2, TRAF5, and HOXA10, influencing the mTOR, TGF-β, and AKT/c-Myc/cyclin D1 pathways (7, 13-15). Likewise, miR-646 has been reported as a tumor suppressor in breast, gastric, colorectal, and osteosarcoma cancers by targeting FOXK1, NOB1, FGF2, and HDAC2, resulting in inhibition of cell proliferation, invasion, and EMT through the TGF-β1-induced EMT and Akt/mTOR pathways (16-19). Despite growing evidence supporting the involvement of these miRNAs in BC and other malignancies, previous studies have largely focused on tissue expression or individual miRNAs in limited cancer stages, whereas their combined circulating expression profiles across all different BC stages remain largely unexplored, particularly in Egyptian patients. Therefore, the present study evaluated the circulating expression of miR-1271-5p, miR-646, and miR-135a-5p across BC stages 0-IV of Egyptian patients and assessed their potential as non-invasive biomarkers for BC diagnosis and staging. In addition, integrative network analyses incorporating validated and predicted targets were performed to explore the putative molecular pathways and regulatory miRNA/lncRNA/mRNA gene networks associated with these miRNAs. The findings could contribute to the identification of novel non-invasive biomarkers for BC diagnosis and staging while providing insight into possible underlying molecular mechanisms.

Materials and methods

Study Population and Design

Prior to conducting this study, estimation of sample size was carried out using G*Power software. The minimum number of samples required to be enrolled in this study was determined using an F-test with the following input parameters: 3 independent groups with a significance level of $\alpha = 0.05$, a medium effect size ($f = 0.25$), a type II error of $\beta = 0.2$, and a population standard deviation ($SD = 0.5$). The minimal total number of participants required to yield 80% statistical power ($1-\beta = 0.8$) was 159 participants. This observational cross-sectional study included 160 Egyptian women recruited consecutively from the Baheya Foundation for Early Detection and Treatment of Breast Cancer between March 7, 2022, and March 6, 2023, comprising 111 BC patients (stages 0-IV), 25 benign breast disease cases, and 24 healthy controls. All participants were >20 years old and provided written informed consent. The study was approved by the Baheya Foundation Ethics Committee (Serial No. 202203070012) and conducted in accordance with the Declaration of Helsinki.

Eligible participants included females with histopathologically confirmed BC at any clinical stage. Patients who had received neoadjuvant chemotherapy or radiotherapy before surgery or had a history of other primary malignancies were excluded. Clinical evaluation included medical history, physical examination, radiological investigations, and PET/CT scans. Tumor staging was determined according to the AJCC 8th edition TNM classification, and molecular subtypes were assigned based on ER, PR, HER2 status, and tumor grade. ER and PR positivity (≥1% positive tumor cell nuclei) and HER2 status were assessed by immunohistochemistry (IHC) (Ventana system), with equivocal (2+) HER2 cases confirmed by silver in situ hybridization (SISH). Histological grading followed the Nottingham grading system, and performance status was assessed using the ECOG criteria.

Plasma Collection and RNA Isolation

Peripheral blood was collected in EDTA tubes, and any sample showing visible hemolysis was excluded from subsequent preparations. Plasma preparation was then conducted within 4 h of blood collection through sequential centrifugation at 4,000 rpm for 10 mins and 13,000 rpm for 10 mins at 4°C to remove cellular debris using the fixed rotor of the PrO-Research centrifuge (Centurion Scientific, UK). Aliquots (200 µL) were stored at −80°C until analysis. Total RNA, including miRNAs, was extracted using the Direct-zol™ RNA MiniPrep Kit (Zymo Research, USA). Synthetic cel-miR-39-3p (Qiagen, Germany) was added at 25 fmol to each plasma sample during RNA extraction as an external spike-in control to monitor RNA extraction efficiency, and RNA concentration and purity were assessed using a NanoDrop spectrophotometer as detailed previously (20-21).

cDNA Synthesis and Quantitative RT-PCR

A total of 100 ng RNA was polyadenylated using E. coli Poly(A) Polymerase (New England Biolabs, UK) and reverse transcribed using the GoScript Reverse Transcription Kit (Promega, USA). Quantitative RT-PCR was performed on a StepOnePlus™ Real-Time PCR System (Applied Biosystems, USA) using GoTaq® qPCR Master Mix (Promega, USA) with miRNA-specific forward primers and a universal reverse primer **(Supplementary Tables, Table S1)**. The optimal annealing temperature for each miRNA target was determined based on melt-curve analysis, with a single distinct peak confirming the specificity of amplification for each target **(Supplementary Figures, Fig. S1).** Relative expression levels were calculated using the $2^{-\Delta\Delta Ct}$ method as described earlier (22-24).

Statistical and Bioinformatic Analyses

Statistical analyses were performed using SPSS v15.0 and GraphPad Prism v5.0. Categorical variables were compared using Chi-square or Fisher's exact tests. Normally distributed variables were analyzed using one-way ANOVA with Tukey's post hoc test, whereas non-normally distributed variables were analyzed using Mann–Whitney U or Kruskal–Wallis tests. Correlations were assessed using Spearman's rank coefficient. Diagnostic performance was evaluated by ROC curve analysis, and relapse predictors were investigated using univariate logistic regression. Statistical significance was considered at a p-value < 0.05. To account for multiple hypothesis testing, p-values obtained from post hoc pairwise comparisons were adjusted using the Benjamini–Hochberg false discovery rate (FDR) correction. Statistical significance was considered at an FDR-adjusted p-value (q-value) <0.05. Predicted miRNA targets were identified using TargetScan and miRDB, while experimentally validated interactions were retrieved through MIENTURNET/miRTarBase. Functional enrichment analyses were performed using KEGG and Reactome databases, and miRNA–lncRNA interaction networks were explored using miRNet.

Results

Clinical Features and Demographics of the Participants

The observed demographic and clinicopathological laboratory profiles, including TNM stage, tumor grade, receptor status, molecular subtype distribution, and metastatic status, confirmed appropriate stratification of patients into their respective BC stages and study groups (Supplementary Tables, Tables S2-S4).

Comparative Levels of miRNAs Between Study Cohorts: A Comparative Study

Compared with healthy controls, benign breast lesions exhibited significant downregulation of miR-1271-5p (p=0.035) and miR-646 (p = 0.002), whereas miR-135a-5p was not significantly different after FDR correction (adjusted p = 0.089). Relative to benign cases, miR-1271-5p was significantly overexpressed in stages 0-III BC (p = 0.023, p = 0.002, p = 0.001, and p = 0.023, respectively), while miR-646 showed significant elevation in stage III (p = 0.001). In contrast, miR-135a-5p was markedly reduced in metastatic stage IV compared with benign lesions (P = 0.005) (Fig. 1). Across BC stages, miR-1271-5p displayed a consistent pattern of overexpression relative to healthy controls, particularly in stages I and II. Conversely, miR-646 was generally downregulated in benign and malignant samples, with a transient increase in stage III. miR-135a-5p was markedly elevated in benign and early-stage disease (stages 0-III) but significantly decreased in stage IV, indicating a potential association with metastatic progression (Fig. 1). Further comparisons among BC stages demonstrated significantly lower miR-646 expression in stages 0 and I than in stage III (p = 0.049 and p = 0.003, respectively). Notably, miR-135a-5p expression was significantly lower in metastatic stage IV than in non-metastatic stages I–III (P = 0.001, p = 0.001, and p = 0.005, respectively), whereas the difference between stages 0 and IV was of marginal significance after Benjamini–Hochberg FDR correction (p = 0.058) (Fig. 1). When patients were grouped according to disease status, miR-1271-5p and miR-135a-5p were significantly elevated in early-stage compared with advanced-stage BC (p = 0.0028 and p = 0.0037, respectively), whereas miR-646 showed the opposite trend (p = 0.0051). Furthermore, combined BC cases displayed significantly increased miR-1271-5p (p = 0.0336) and miR-135a-5p expression (p = 0.0277) and reduced miR-646 expression (p = 0.0169) relative to healthy controls, supporting their potential utility as diagnostic and stage-associated biomarkers (Supplementary Figures, Figs S2-S4)

Plasma miRNAs' Diagnostic Accuracy

ROC curve analyses demonstrated distinct diagnostic and stage-specific performance for the investigated miRNAs (Table 1). Among all markers, miR-135a-5p showed the strongest ability to identify metastatic disease (Stage IV), distinguishing Stage IV from all stages, including healthy controls, non-metastatic stages (0-III stages), and benign cases with consistently high sensitivity (90%) and specificity values ranging from 75 to 100%.

Furthermore, miR-646 demonstrated the best performance in identifying Stage III disease, effectively differentiating Stage III from benign cases and also non-malignant stages (0-II stages) with AUC ranging from 0.75 to 0.85. Moreover, miR-646 could accurately distinguish healthy controls from both benign cases and Stage I (Table 1). On the other hand, miR-1271-5p exhibited excellent discriminatory power for Stage II disease against all other stages with an AUC range of 0.764-0.938.

For early disease detection, miR-135a-5p showed the highest performance in distinguishing Stage 0 from healthy controls (AUC = 0.857), while miR-646 and miR-1271-5p also demonstrated good diagnostic accuracy in differentiating Stage I and Stage II disease from healthy and benign groups (Table 1). When all BC stages were combined, each miRNA significantly discriminated BC patients from healthy controls (AUC 0.667–0.680). Furthermore, all three miRNAs differentiated early-stage (0–II) from advanced-stage (III–IV) disease, with miR-135a-5p showing the highest performance (AUC=0.722), followed by miR-1271-5p (AUC = 0.715) and miR-646 (AUC = 0.689) (Table 1). Notably, miR-1271-5p effectively distinguished malignant from non-malignant cases (AUC = 0.744) and benign cases from combined BC stages (AUC = 0.831), whereas miR-646 and miR-135a-5p successfully differentiated healthy controls from breast tumors (benign and malignant combined), achieving AUC values of 0.705 and 0.671, respectively.

Logistic regression analysis of miRNAs

Logistic regression analyses identified significant associations between the investigated miRNAs and BC diagnosis and staging (Supplementary Tables, Tables S5-S6). Univariate analysis showed that miR-1271-5p was significantly downregulated in benign cases compared with healthy controls (OR = 0.0376, 95% CI: 0.0026-0.5486, p = 0.016) and early-stage BC

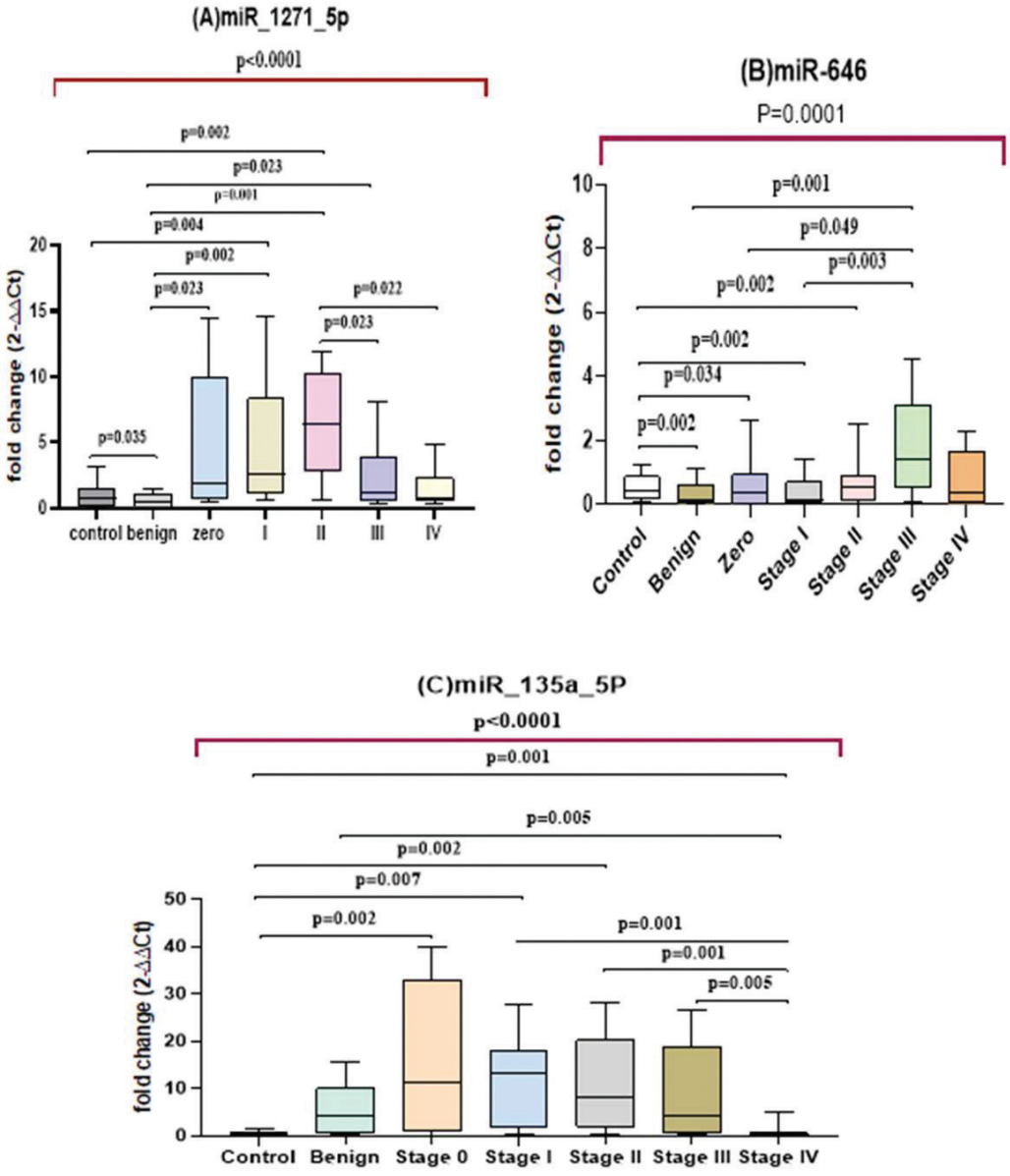

FIGURE 1 - Plasma miRNA expression levels of (A) miR-1271-5p, (B) miR-646, and (C) miR-135a-5p among healthy controls, benign, and BC patients from stage 0 to stage IV (0-IV). Each box plot illustrates the distribution of fold change with the interquartile range (25th-75th percentiles), a line representing the median, and whiskers indicating the 10th and 90th percentiles. Pairwise P values were Benjamini–Hochberg FDR-adjusted.

TABLE 1 - Summarizes the diagnostic accuracy of the plasma miRNAs examined in distinguishing healthy controls, benign conditions, and the various stages of BC (0-IV). p ≤ 0.05 is significant, whereas p>0.05 is not significant

miRNAs	P value	AUC	Sensitivity %	Specificity%	Std. Error	95% confidence interval	best cutoff
miR-1271-5P							
Control vs Benign (24 vs 25)	0.0246	0.7333	73.33	100	0.1142	0.5095-0.9571	<0.9450
Control vs Stage I (24 vs 30)	0.0022	0.8125	81.25	100	0.09758	0.6213-1.000	>1.030
Control vs II (24 vs 23)	0.0007	0.8571	85.71	100	0.09352	0.6738-1.000	>1.485
Stage Zero vs Benign (15 vs 25)	0.008	0.8296	66.67	86.67	0.08782	0.6575-1.000	>1.258
Stage I vs Benign (30 vs 25)	0.0005	0.8667	62.5	86.67	0.06312	0.7430-0.9904	>1.305
Stage II vs Benign (23 vs 25)	<0.0001	0.9381	85.71	93.33	0.04593	0.8481-1.000	>1.425
Stage II vs III (23 vs 28)	0.0096	0.7643	85	57.14	0.08204	0.6035-0.9251	<5.835

miRNAs	P value	AUC	Sensitivity %	Specificity%	Std. Error	95% confidence interval	best cutoff
Stage II vs IV (23 vs 15)	0.009	0.8571	85.71	78.57	0.08343	0.6936-1.000	<2.646
Stage III vs Benign (28 vs 25)	0.0063	0.7733	100	46.67	0.0801	0.6163-0.9303	>0.3095
Control vs total BC cases (24 vs 111)	0.0349	0.667	66.67	100	0.05803	0.5529-0.7804	>1.030
Early stages vs Late stages (68 vs 43)	0.0031	0.7151	88.89	43.59	0.06287	0.5919-0.8383	<5.835
Non-malignant vs Malignant (49 vs 111)	<0.0001	0.7438	60.61	93.75	0.0501	0.6457-0.8420	>1.258
Benign vs total BC cases (25 vs 111)	<0.0001	0.8313	90.91	53.33	0.05346	0.7265-0.9361	>0.5160
miR-646							
Control vs Benign (24 vs 25)	0.0011	0.8235	82.35	100	0.09246	0.6423-1.000	<0.9250
Control vs 0 (24 vs 15)	0.0223	0.75	75	100	0.125	0.5050-0.9950	<0.9068
Control vs Stage I (24 vs 30)	0.0002	0.85	85	100	0.07984	0.6935-1.000	<0.8550
Control vs II (24 vs 23)	0.0011	0.8235	82.35	100	0.09246	0.6423-1.000	<0.9600
Stage Zero vs III (15 vs 28)	0.0176	0.7542	65	83.33	0.09135	0.5751-0.9332	>1.009
Stage I vs III (30 vs 28)	0.001	0.805	65	85	0.06849	0.6708-0.9392	>0.8650
Stage II vs III (23 vs 28)	0.0214	0.7221	65	76.47	0.08503	0.5554-0.8887	>0.9100
Stage III vs Benign (28 vs 25)	0.0002	0.8574	80	76.47	0.05976	0.7402-0.9745	>0.4550
Control vs total BC cases (24 vs 111)	0.018	0.680	67.95	100	0.05284	0.5759-0.7831	<0.9600
Early stages vs Late stages (68 vs 43)	0.0055	0.689	55.17	69.39	0.06344	0.5646-0.8133	>0.7050
Control vs Breast tumors (24 vs 136)	0.0059	0.7053	70.53	100	0.04678	0.6136-0.7969	<0.9600
miR-135a-5p							
Control vs 0 (24 vs 15)	0.006	0.8571	85.71	100	0.1323	0.5979-1.000	>1.058
Control vs Stage I (24 vs 30)	0.0067	0.7647	76.47	100	0.1029	0.5631-0.9663	>2.037
Control vs II (24 vs 23)	0.001	0.8462	84.62	100	0.1001	0.6500-1.000	>1.309
Control vs IV (24 vs 15)	0.0005	0.9	90	100	0.09487	0.7141-1.000	<0.8620
Stage Zero vs IV (15 vs 15)	0.0248	0.8286	90	85.71	0.1327	0.5684-1.000	<0.9250
Stage I vs IV (30 vs 15)	0.0002	0.9353	90	82.35	0.04521	0.8467-1.000	<0.7775
Stage II vs IV (23 vs 15)	0.0006	0.9231	90	84.62	0.05626	0.8128-1.000	<1.176
Stage III vs IV (28 vs 15)	0.0024	0.8769	90	84.62	0.07696	0.7261-1.000	<0.7399
IV vs Benign (15 vs 25)	0.0027	0.8563	90	75	0.07808	0.7032-1.000	<0.8475
Control vs total BC cases (24 vs 111)	0.0293	0.667	66.67	100	0.06086	0.5474-0.7859	>1.058
Early stages vs Late stages (68 vs 43)	0.0042	0.7215	65.22	75.68	0.06991	0.5845-0.8585	<1.563
Non-Metastatic vs Metastatic (96 vs15)	<0.0001	0.902	90	84	0.04702	0.8098-0.9942	<0.7399
Control vs Breast tumors (24 vs 136)	0.0216	0.6711	67.11	100	0.05389	0.5654-0.7767	>1.058

cases, while its expression was significantly higher in combined BC cases than in benign lesions (OR = 4.5643, 95% CI: 1.2514-16.6469, p = 0.0215). Moreover, miR-1271-5p expression declined in Stage III relative to Stage II disease (OR = 0.7588, 95% CI: 0.6079-0.9472, p = 0.0147), suggesting stage-dependent variation.

miR-646 was markedly reduced in benign (OR = 0.0036, 95% CI: 0.00007-0.1897, p = 0.0054) and Stage I cases (OR = 0.0134, 95% CI: 0.0008-0.2243, p = 0.0027) compared with healthy controls, indicating early dysregulation during disease development. In contrast, Stage III patients exhibited significantly higher miR-646 levels than Stage I groups (OR = 5.1220, 95% CI: 1.4514-18.0757, p = 0.0111) and benign cases. miR-135a-5p was significantly elevated in Stage I relative to benign cases (OR = 0.8941, 95% CI: 0.8056-0.9922, p = 0.0352) and showed a modest but significant increase in tumor-bearing individuals compared with healthy controls (OR = 1.4670, 95% CI: 1.0154-2.1195, p = 0.0412) (Supplementary Tables, Tables S5-S6).

Stepwise multivariate analysis demonstrated that a combined three-miRNA panel (miR-1271-5p, miR-646, and miR-135a-5p) effectively differentiated early-stage (0-II) from advanced-stage (III-IV) BC, achieving an AUC of 0.763, with 75.9% sensitivity and 63.3% specificity (Table 6). Furthermore, a two-miRNA panel comprising miR-1271-5p and miR-135a-5p significantly distinguished malignant from non-malignant breast conditions, yielding an AUC of 0.701, 62.8% sensitivity, and 94.4% specificity (Supplementary Tables, Tables S5-S6).

To assess the potential confounding effect of age, additional age-adjusted binary logistic regression analyses were performed for the principal diagnostic comparisons (Supplementary Table S7). After adjustment, miR-1271-5p remained significantly associated with BC compared with both healthy controls (OR = 2.092, 95% CI: 1.043-4.196, p = 0.038) and benign breast disease (OR = 4.271, 95% CI: 1.152-15.839, p = 0.030). Moreover, miR-646 was also independently associated with BC compared with benign breast disease (OR = 3.656, 95% CI: 1.050-12.735, p = 0.042), whereas miR-135a-5p remained significantly associated only in the comparison between healthy controls and BC (OR = 1.406, 95% CI: 1.002-1.975, p = 0.049).

Prognostic Significance of miR-1271-5p, miR-646, and miR-135a-5p in the Prediction of BC Recurrence

Univariate logistic regression identified several significant predictors of BC recurrence (Supplementary Tables, Table S8). Among the investigated miRNAs, miR-1271-5p was inversely associated with recurrence risk (OR = 0.843, 95% CI: 0.722-0.985, p = 0.032), suggesting a potential protective role, whereas elevated miR-646 levels were associated with increased relapse risk (OR = 1.880, 95% CI: 1.164-3.038, p = 0.0099). Clinicopathological factors significantly linked to recurrence included invasive ductal carcinoma (IDC; OR = 9.333, 95% CI: 1.165-74.760, p = 0.035), advanced disease stage (≥III; OR = 21.412, 95% CI: 2.573-178.181, p = 0.0046), and larger tumor size (T3: OR = 11.846, 95% CI: 1.337-104.991, p = 0.026; T4: OR = 10.769, 95% CI: 1.205-96.212, p = 0.033). Conversely, positive ER (OR = 0.180, 95% CI: 0.070-0.461, p < 0.001) and PR status (OR = 0.223, 95% CI: 0.090-0.551, p = 0.001) were significantly associated with reduced recurrence risk. No significant associations were observed for miR-135a-5p, age, parity, menstrual status, family history, BMI, ECOG status, nodal status, or HER2 expression.

Association analyses between circulating miRNA levels and clinical parameters

Association analyses showed that miR-646 expression was significantly associated with higher tumor grade (p = 0.013) and disease relapse (p = 0.0057). In contrast, miR-135a-5p levels were significantly reduced with increasing lymph node involvement (p = 0.0070) and in metastatic disease (p < 0.0001). miR-1271-5p showed a borderline association with progression status, with higher expression in non-relapsing patients (p = 0.0505) (Supplementary Tables, Table S9).

Computational & Functional Annotation with Enrichment Analysis of miRNA-Target Networks

Functional target analysis using experimentally validated interactions from miRTarBase identified regulatory networks for miR-1271-5p, miR-646, and miR-135a-5p. KEGG enrichment revealed significant associations of miR-1271-5p with cancer-related pathways, including AMPK, FoxO, thyroid hormone signaling, and AGE–RAGE signaling, whereas miR-135a-5p and miR-646 showed no significant KEGG enrichment. Reactome analysis demonstrated significant enrichment of miR-135a-5p targets in FOXO regulation, IL-4/IL-13 signaling, AGE receptor signaling, and TP53-mediated cell death pathways, while miR-646 was enriched in SUMOylation of DNA replication proteins (Fig. 2).

Computational Prediction of miRNA Targets

According to the Target Scan and miRDB prediction tools, miR-1271-5p, miR-646, and miR-135a-5p primarily target genes associated with benign tumors and BC development and progression. We carefully examined the potential targets for the selected miRNAs to explain the significance of the dysregulation of their expression in the context of BC progression. The assumed targets for miR-1271-5p are *SPIN1* (spindlin 1); *HAS2* (hyaluronan synthase 2); *ITPR1* (inositol 1,4,5-trisphosphate receptor type 1); *MTSS1* (MTSS1, I-BAR domain containing); *CTTN* (cortactin) and ZEB1(zinc finger E-box binding homeobox 1). The predicted targets for miR-646 are *EphB2* (EPH receptor B2); *NKD1* (NKD1, WNT signaling pathway inhibitor); *CCND2* (cyclin D2), and *INSR* (insulin receptor). The putative targets for miR-135a-5p are *FOXN3* (forkhead box N3); *DIP2C* (disco interacting protein 2 homolog C); *RUNX2* (runt related transcription factor 2); *YWHAG* (tyrosine 3-monooxygenase/tryptophan 5-monooxygenase activation protein gamma), and *RASAL2* (RAS protein activator like 2). Target prediction analysis for the examined miRNAs is summarized in (Supplementary Tables, Table S10).

Computational and bioinformatics identification of miRNA–lncRNA interaction

A network-based identification tool for miRNA–long non-coding RNA (lncRNA) interaction was constructed using

miRNet software (Chang et al., 2020). Five (long non-coding RNA) lncRNAs, including *HCG18* (HLA Complex Group 18), *TP53TG1* (TP53 target 1), *NNT-AS1*(NNT antisense RNA 1), *UCA1* (Urothelial Carcinoma-Associated 1), and *LINC02381* (Long Intergenic Non-Protein Coding RNA 2381), were identified to interact with miR-1271-5p. Additionally, another five lncRNAs, including *GAS5* (Growth Arrest-Specific 5), *LINC00852*, *LINC01087*, *DANCR* (Differentiation Antagonizing Non-Protein Coding RNA), and *NEAT1* (Nuclear Enriched Abundant Transcript 1), were identified to have the possibility of interacting with miR-135a-5p. At the same time, three lncRNAs: *ZFAS1* (Zinc Finger Antisense 1), *XIST* (X Inactive Specific Transcript), and *MALAT1* (Metastasis-Associated Lung Adenocarcinoma Transcript 1) were identified to have a common interaction with both miR-1271-5p and miR-135a-5p, as shown in Figure 3.

Discussion

Despite advances in BC screening, up to 20% of patients are still diagnosed at advanced stages, highlighting the need for more accurate early detection tools. Circulating miRNAs are stable, non-invasive biomarkers with established roles in cancer biology and diagnosis (25-26). Their expression profiles can be reliably assessed using techniques such as RT-qPCR, microarrays, and RNA sequencing, making them promising candidates for BC detection and monitoring (27-32). This study evaluated, for the first time to our knowledge, the circulating expression profiles of miR-1271-5p, miR-646, and miR-135a-5p in an Egyptian cohort comprising benign breast disease and BC stages 0–IV and explored their potential biological relevance through integrative bioinformatic analyses. Distinct stage-specific expression patterns were observed, with miR-1271-5p and miR-135a-5p predominantly elevated in early-stage disease, miR-646 showing a transient increase in stage III, and miR-135a-5p markedly reduced in metastatic stage IV. ROC analyses demonstrated promising diagnostic performance, while bioinformatic analyses identified cancer-related targets, signaling pathways, and regulatory lncRNA–miRNA–mRNA networks, suggesting the potential biological relevance of these miRNAs.

Although previous studies have largely described miR-1271-5p as a tumor suppressor in several malignancies, such as HCC and ovarian cancer (33-34), its plasma circulatory levels were significantly downregulated in benign tumors but upregulated across all BC stages. Additionally, its precursor form, miR-1271, has also been reported to be downregulated in BC tissues and cell lines (35). Interestingly, our findings revealed elevated plasma levels despite reports of reduced expression for its precursor, miR-1271 (35), in BC tissues, highlighting the well-recognized discrepancy between circulating and tissue-derived miRNAs. Such differences may result from active secretion through extracellular vesicles or passive release from damaged or apoptotic cells. In addition, selective exosomal secretion, altered intracellular retention, differential miRNA stability, and tumor–host interactions

A

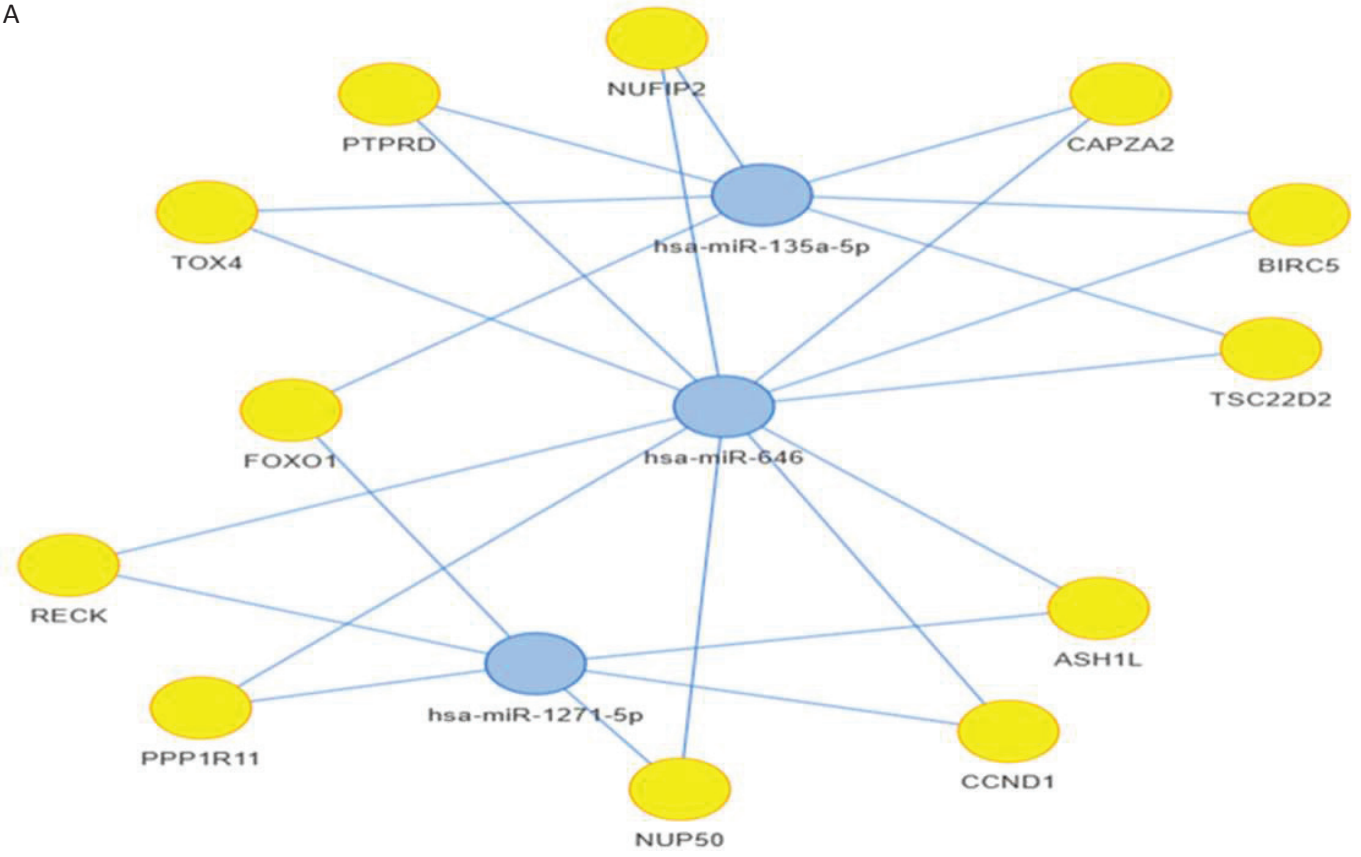

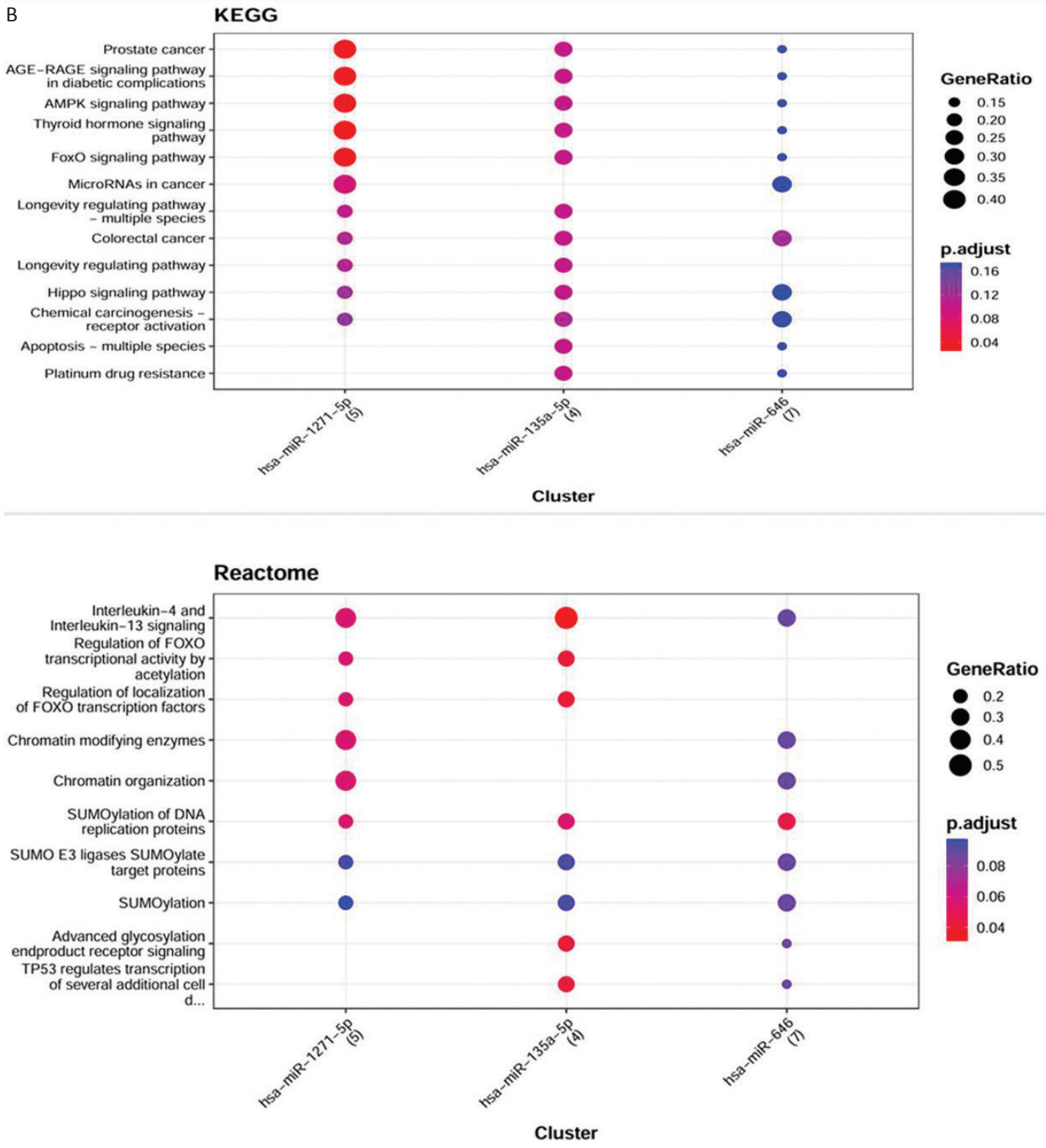

FIGURE 2 - Shows the output of the MIENTURNET tool with the selected miRNAs (hsa-miR-1271-5p, hsa-miR-646, and hsa-miR-135a-5p): (A) A plot of miRNA-target gene interactions based on miRTarBase, where miRNAs are represented as blue nodes, and their target genes are represented as yellow nodes. (B) Dot plot of KEGG and Reactome pathway enrichment analysis of the miRNA target genes. Annotation terms (e.g., biological pathways) on the Y-axis and miRNAs on the X-axis. Dot size = number of involved genes, and dot color = adjusted p-value (FDR).

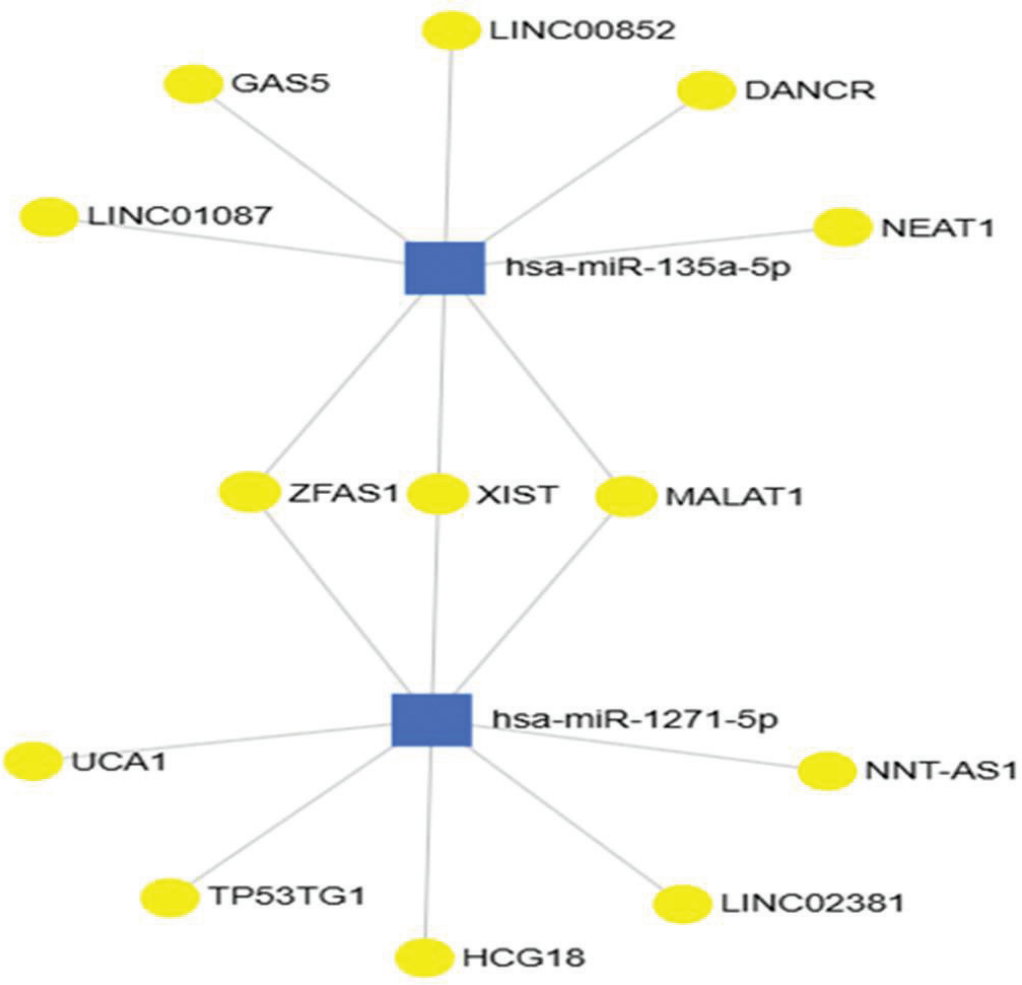

FIGURE 3 - Presents the miRNA–lncRNA interaction, where yellow dots represent long non-coding RNAs and blue triangles represent miRNAs of interest.

may also contribute to this discrepancy (36-37). Therefore, circulating miRNA levels may not necessarily reflect their expression within tumor tissues and should be interpreted cautiously. Integrative analyses identified several experimentally validated and predicted targets involved in cancer progression, including *RECK, CCND1, ZEB1, SPIN1, HAS2, MTSS1,* and *CTTN***.** These genes are associated with EMT, proliferation, invasion, and metastasis, suggesting a potential role for miR-1271-5p in BC progression. Network analysis further identified lncRNAs such as *TP53TG1* and *LINC02381* as potential interaction partners, suggesting broader regulatory networks that warrant experimental validation.

On the other hand, miR-646 exhibited a unique expression pattern, being downregulated in benign tumors and most BC stages but elevated specifically in stage III disease. Previous studies have generally described miR-646 as a tumor suppressor in breast cell lines (17), as well as in other cancers, including lung cancer (38) and colorectal cancer (16), which is consistent with our results, especially in early stages of BC. The stage III-specific increase may reflect context-dependent regulation during disease progression. One possible explanation involves the TET1 pathway, which exhibits distinct functions under normoxic and hypoxic conditions. Changes in tumor oxygenation during progression and dissemination could influence miR-646 expression; however, this hypothesis remains speculative and requires functional validation. Bioinformatic analyses identified validated targets including *TSC22D2, PTPRD, TOX4,* and *BIRC5,* together with predicted targets such as *EphB2, NKD1, INSR,* and *CCND2***.** These genes participate in cell-cycle regulation, EMT, proliferation, and metastatic dissemination, suggesting the potential involvement of miR-646 in tumor progression.

Moreover, miR-135a-5p showed elevated expression in benign tumors and early-stage BC (stages 0-III), followed by marked suppression in metastatic stage IV disease. Furthermore, lower miR-135a-5p levels were associated with lymph node involvement and distant metastasis. These findings are consistent with previous reports suggesting a tumor-suppressive role in gastric and prostate cancers for miR-135a-5p and its association with advanced disease and metastatic progression (39-40). The pronounced reduction observed in stage IV patients, together with its strong diagnostic performance, indicates potential utility in distinguishing metastatic from non-metastatic disease.

Bioinformatic putative analyses identified *FOXO1* as a validated target shared by miR-1271-5p and miR-135a-5p. *FOXO1* is a key tumor suppressor involved in apoptosis, cell-cycle arrest, and oxidative stress regulation. Enrichment analyses suggested potential associations between these miRNAs and FOXO signaling pathways, while miR-1271-5p was additionally associated with AMPK signaling. Both pathways are recognized regulators of cellular metabolism, proliferation, and survival in BC, suggesting potential mechanistic relevance of the identified miRNA signatures that warrants further experimental validation.

Additional predicted targets of miR-135a-5p included *FOXN3* and *RUNX2*, genes implicated in EMT, invasion, and metastatic progression. Network analyses also identified several candidate lncRNA interactions, including *GAS5, DANCR, NEAT1, ZFAS1, XIST,* and *MALAT1.* These lncRNAs have established roles in tumor growth, invasion, metastasis, and regulation of signaling pathways relevant to BC. Notably, *ZFAS1, XIST, and MALAT1* were predicted to interact with both miR-1271-5p and miR-135a-5p, suggesting possible convergence within shared regulatory networks; however, these predicted interactions require experimental validation.

This study has several limitations, including the relatively small benign and healthy control groups and the single-center design, which may limit the generalizability of the findings. ROC analyses involving small subgroups may overestimate diagnostic performance, and the findings require validation in larger independent multicenter cohorts with internal and external validation. Furthermore, the cellular origin of the circulating miRNAs could not be determined, and the predicted pathways and regulatory networks require further experimental validation.

Conclusion

Collectively, the present findings demonstrate distinct stage-dependent expression patterns of circulating miR-1271-5p, miR-646, and miR-135a-5p in BC. Their diagnostic performance, particularly when combined into multi-miRNA panels, supports their potential utility as minimally invasive biomarkers for BC detection and staging. Integrative analyses further suggest involvement of cancer-related pathways, including AMPK, FOXO, TP53-mediated cell death, immune signaling, and SUMOylation processes, together with putative regulation of genes such as ZEB1, CCND2, FOXN3, and RUNX2. However, the mechanistic conclusions derived from bioinformatic analyses should be interpreted cautiously until validated experimentally. Further multicenter studies and functional investigations are warranted to validate these findings and confirm the clinical and biological relevance of the identified miRNAs in BC.

Disclosures

Conflict of interest: The authors declare that they have no competing interests

Financial support: This research received no specific grant from any funding agency in the public, commercial, or not-for-profit sectors.

Authors' contributions: AAYG, ARA and DMA conceived and designed the experiments. MMM provided samples, recruited patients, and provided some of the patients' clinical data. MB and AAYG performed experimental work in addition to statistical, bioinformatics, and network analyses. AAYG designed primers for this study. MB and AAYG drafted the manuscript. AAYG, MMM, DMA, MB and ARA revised and approved the manuscript.

Data availability statement: All data generated or analysed during this study are included in this published article and its supplementary information files.

Ethics approval and consent to participate: This study followed the ethical principles outlined in the Helsinki Declaration and was approved by the Baheya Foundation Ethics Committee (Serial: 202203070012), and written informed consent was collected from all participating individuals before participating in the study.

References

1. Bray F, Laversanne M, Sung H, et al. Global cancer statistics 2022: GLOBOCAN estimates of incidence and mortality worldwide for 36 cancers in 185 countries. CA Cancer J Clin. 2024;74(3):229-263. CrossRef PubMed
2. Abdel-Fadeel NA, Zanaty MM, Kamal AM, et al. Childhood psychological trauma and psychiatric comorbidity in patients with breast cancer. Egypt J Hosp Med. 2022;88(1):2788-2794. CrossRef
3. Santiago L, Adrada BE, Huang ML, et al. Breast cancer neoplastic seeding in the setting of image-guided needle biopsies of the breast. Breast Cancer Res Treat. 2017;166(1):29-39. CrossRef PubMed
4. Shao Y, Sun X, He Y, et al. Elevated levels of serum tumor markers CEA and CA15-3 are prognostic parameters for different molecular subtypes of breast cancer. PLoS One. 2015;10(7):e0133830. CrossRef PubMed
5. El-Maraghy SA, Adel O, Zayed N, et al. Circulatory miRNA-484, 524, 615 and 628 expression profiling in HCV mediated HCC among Egyptian patients; implications for diagnosis and staging of hepatic cirrhosis and fibrosis. J Adv Res. 2019;22:57-66. CrossRef PubMed
6. Gibriel AA, Ismail MF, Sleem H, et al. Diagnosis and staging of HCV associated fibrosis, cirrhosis and hepatocellular carcinoma with target identification for miR-650, 552-3p, 676-3p, 512-5p and 147b. Cancer Biomark. 2022;34(3):413-430. CrossRef PubMed
7. Zhang H, Wang M, Lang Z, et al. MiR-135a-5p suppresses breast cancer cell proliferation, migration, and invasion by regulating BAG3. Clinics (Sao Paulo). 2022;77:100115. CrossRef PubMed
8. Bahar NAA, Al-Ouqaili MTS, Talib NM. Improving the diagnosis and follow-up of chronic myeloid leukemia using conventional and molecular techniques. J Clin Lab Anal. 2025;39(5):e70001. CrossRef PubMed
9. Fan G, Jiao J, Shen F, et al. Upregulation of lncRNA ZFAS1 promotes lung adenocarcinoma progression by sponging miR-1271-5p and upregulating FRS2. Thorac Cancer. 2020;11(8):2178-2187. CrossRef PubMed
10. Wang Y, Wang Z, Cheng K, et al. FAM201A promotes cervical cancer progression and metastasis through miR-1271-5p/flotillin-1 axis targeting-induced Wnt/β-catenin pathway. J Oncol. 2022;2022:1123839. CrossRef PubMed
11. Liu N, Feng S, Li H, et al. Long non-coding RNA MALAT1 facilitates the tumorigenesis, invasion and glycolysis of multiple myeloma via miR-1271-5p/SOX13 axis. J Cancer Res Clin Oncol. 2020;146(2):367-379. CrossRef PubMed
12. Zhang B, Chen J, Cui M, et al. LncRNA ZFAS1/miR-1271-5p/HK2 promotes glioma development through regulating proliferation, migration, invasion and apoptosis. Neurochem Res. 2020;45(12):2828-2839. CrossRef PubMed

13. Diao H, Xu X, Zhao B, et al. miR-135a-5p inhibits tumor invasion by targeting ANGPT2 in gallbladder cancer. Mol Med Rep. 2021;24(1):528. CrossRef PubMed
14. Guo LM, Ding GF, Xu W, et al. MiR-135a-5p represses proliferation of HNSCC by targeting HOXA10. Cancer Biol Ther. 2018;19(11):973-983. CrossRef PubMed
15. Luo W, Sun C, Zhou J, et al. miR-135a-5p functions as a glioma proliferation suppressor by targeting tumor necrosis factor receptor-associated factor 5 and predicts patients' prognosis. Am J Pathol. 2019;189(1):162-176. CrossRef PubMed
16. Dai H, Hou K, Cai Z, et al. Low-level miR-646 in colorectal cancer inhibits cell proliferation and migration by targeting NOB1 expression. Oncol Lett. 2017;14(6):6708-6714. CrossRef PubMed
17. Darvishi N, Rahimi K, Mansouri K, et al. MiR-646 prevents proliferation and progression of human breast cancer cell lines by suppressing HDAC2 expression. Mol Cell Probes. 2020;53:101649. CrossRef PubMed
18. Sun XH, Geng XL, Zhang J, et al. miRNA-646 suppresses osteosarcoma cell metastasis by downregulating fibroblast growth factor 2 (FGF2). Tumor Biology. 2015;36(3):2127–2134 CrossRef
19. Zhang P, Tang WM, Zhang H, et al. MiR-646 inhibited cell proliferation and EMT-induced metastasis by targeting FOXK1 in gastric cancer. Br J Cancer. 2017;117(4):525-534. CrossRef PubMed
20. Gibriel AA, Abou-Elew MH, Masmoudi S. Analysis of p.Gly12 Valfs*2, p.Trp24* and p.Trp77Arg mutations in GJB2 and p.Arg 81Gln variant in LRTOMT among non syndromic hearing loss Egyptian patients: implications for genetic diagnosis. Mol Biol Rep. 2019;46(2):2139-2145. CrossRef PubMed
21. Gibriel AAY, Tate RJ, Yu Y, et al. The p.Arg86Gln change in GARP2 (glutamic acid-rich protein-2) is a common West African-related polymorphism. Gene. 2013;515(1):155-158. CrossRef PubMed
22. Schmittgen TD. Real-time quantitative PCR. Methods. 2001;25(4): 383-385. CrossRef PubMed
23. Shatta MA, El-Derany MO, Gibriel AA, El-Mesallamy HO. Rhamnetin ameliorates non-alcoholic steatosis and hepatocellular carcinoma in vitro. Mol Cell Biochem. 2023;478(8):1689-1704. CrossRef PubMed
24. Abo-Salem HM, Gibriel AA, El Awady ME, et al. Synthesis, molecular docking and biological evaluation of novel flavone derivatives as potential anticancer agents targeting Akt. Med Chem. 2021;17(2):158-170. CrossRef PubMed
25. Sochor M, Basova P, Pesta M, et al. Oncogenic microRNAs: miR-155, miR-19a, miR-181b, and miR-24 enable monitoring of early breast cancer in serum. BMC Cancer. 2014;14(1):448. CrossRef PubMed
26. Gibriel AA, Al-Anany AM, Al-Arab MAE, Azzazy HME. Investigating circulatory microRNA expression profiles in Egyptian patients infected with hepatitis C virus mediated hepatic disorders. Meta Gene. 2020;26:100792. CrossRef
27. Abdulrazaq ZA, Al-Ouqaili MTS, Talib NM. The impact of circulating 25-hydroxyvitamin D and vitamin D receptor variation on leukemia-lymphoma outcome: molecular and cytogenetic study. Saudi J Biol Sci. 2024;31(1):103882. CrossRef PubMed
28. Bahar NAHA, Al-Ouqaili MTS, Talib NM. Molecular, cytogenetic, and hematological monitoring and response to treatment for chronic myeloid leukemia patients. Al- Anbar Med J (Ft Sam Houst, Tex). 2024;20(2):218-223. CrossRef
29. Abdulrazaq ZA, Salih Al-Ouqaili MT, Talib NM. Association between circulating 25-hydroxy vitamin D receptor and molecular response in multiple myeloma. Pak J Biol Sci. 2023;26(9): 472-481. CrossRef PubMed
30. Ben Ayed I, Ouarda W, Frikha F, et al. SRD5A3-CDG: 3D structure modeling, clinical spectrum, and computer-based dysmorphic facial recognition. Am J Med Genet A. 2021;185(4):1081-1090. CrossRef PubMed
31. Gibriel AAY. Options available for labelling nucleic acid samples in DNA microarray-based detection methods. Brief Funct Genomics. 2012;11(4):311-318. CrossRef PubMed
32. Lyu L, Wang M, Zheng Y, et al. Overexpression of fam234b predicts poor prognosis in patients with luminal breast cancer. Cancer Manag Res. 2020;12:12457-12471. CrossRef PubMed
33. Lin MF, Yang YF, Peng ZP, et al. FOXK2, regulated by miR-1271-5p, promotes cell growth and indicates unfavorable prognosis in hepatocellular carcinoma. Int J Biochem Cell Biol. 2017;88:155-161. CrossRef PubMed
34. Han FJ, Li J, Shen Y, et al. microRNA-1271-5p/TIAM1 suppresses the progression of ovarian cancer through inactivating Notch signaling pathway. J Ovarian Res. 2020;13(1):110. CrossRef PubMed
35. Du HY, Liu B. MiR-1271 as a tumor suppressor in breast cancer proliferation and progression via targeting SPIN1. Eur Rev Med Pharmacol Sci. 2018;22(9):2697-2706. CrossRef PubMed
36. Turchinovich A, Weiz L, Burwinkel B. Extracellular miRNAs: the mystery of their origin and function. Trends Biochem Sci. 2012;37(11):460-465. CrossRef PubMed
37. Yu X, Odenthal M, Fries JWU. Exosomes as miRNA carriers: formation–function–future. Int J Mol Sci. 2016;17(12): 2028. CrossRef
38. Pan Y, Chen Y, Ma D, et al. miR-646 is a key negative regulator of EGFR pathway in lung cancer. Exp Lung Res. 2016;42(6):286-295. CrossRef PubMed
39. Zhang Z, Ren L, Zhao Q, et al. TRPC1 exacerbate metastasis in gastric cancer via ciRS-7/miR-135a-5p/TRPC1 axis. Biochem Biophys Res Commun. 2020e;529(1):85-90. CrossRef PubMed
40. Pan J, Xu X, Wang G. lncRNA ZFAS1 is involved in the proliferation, invasion and metastasis of prostate cancer cells through competitively binding to miR-135a-5p. Cancer Manag Res. 2020;12:1135-1149. CrossRef PubMed